

# Synergistic prognostic implications of left ventricular mechanical dyssynchrony and impaired cardiac sympathetic nerve activity in heart failure patients with reduced left ventricular ejection fraction

Takahiro Doi<sup>1\*</sup>, Tomoaki Nakata<sup>2</sup>, Satoshi Yuda<sup>3</sup>, and Akiyoshi Hashimoto<sup>3</sup>

<sup>1</sup>Department of Cardiology, Obihiro-Kosei General Hospital, W6-S8-1, Obihiro, Hokkaido, 81-080-0016, Japan; <sup>2</sup>Department of Cardiology, Hakodate Goryokaku Hospital, Goryokaku cho 38-3, Hakodate, Hokkaido, 81-040-8611, Japan; and <sup>3</sup>Department of Cardiology, Renal and Metabolic Medicine, Sapporo Medical University, Chuo-ku S1-W16-291, Sapporo, Hokkaido, 81-060-8543, Japan

Received 14 November 2016; editorial decision 22 December 2016; accepted 26 December 2016; online publish-ahead-of-print 30 January 2017

## Aims

Impairment of cardiac sympathetic innervation is a potent prognostic marker in heart failure, while left ventricular mechanical dyssynchrony (LVMD) has recently been noted as a novel prognosis determinant in heart failure patients with reduced LV ejection fraction (HFrEF). This study was designed to determine the correlation between cardiac sympathetic innervation quantified by metaiodobenzylguanidine (MIBG) activity and LVMD measured by electrocardiogram-gated myocardial perfusion imaging and to evaluate their incremental prognostic values in HFrEF patients.

## Methods and results

A total of 570 consecutive HFrEF patients were followed up for 19.6 months with a primary endpoint of lethal cardiac events (CE) such as sudden cardiac death, death due to pump failure and appropriate ICD shock against life-threatening ventricular tachyarrhythmias. Cardiac sympathetic function and innervation were quantified as heart-to-mediastinum ratio (HMR) and washout kinetics of cardiac MIBG activity. LVMD was assessed by a standard deviation (SD) of systolic phase angle in gated myocardial perfusion imaging. Patients with CE ( $n = 166$ , 29%) had a significantly lower HMR and a significantly greater phase SD than did non-CE patients:  $1.46 \pm 0.28$  vs.  $1.63 \pm 0.29$ ,  $P < 0.0001$  and  $39.1 \pm 11.6$  vs.  $33.1 \pm 10.1$ ,  $P < 0.0001$ , respectively. Compared to the single use of optimal cut-offs of late HMR (1.54) and phase SD (38), their combination more precisely discriminated high-risk or low-risk patients from others with log rank values from 7.78 to 65.2 ( $P = 0.0053$  to  $P \leq 0.0001$ ). Among significant univariate variables, multivariate Cox proportional hazards model identified NYHA functional class, estimated glomerular filtration rate (eGFR), HMR 1.54 and phase SD 60 as significant determinants of CE with hazard ratios of 3.108 (95% CI, 2.472–3.910;  $P < 0.0001$ ), 0.988 (95% CI, 0.981–0.996;  $P = 0.0021$ ), 0.257 (95% CI, 0.128–0.498;  $P < 0.0001$ ) and 1.019 (95% CI, 1.019–1.037;  $P = 0.0228$ ), respectively. By combining the four independent determinants, the prognostic powers synergistically ( $P < 0.0001$ ) increased maximally to 263.8.

## Conclusions

Left ventricular mechanical dyssynchrony and impairment of cardiac sympathetic innervation are synergistically related to lethal cardiac events, contributing to better stratification of lethal cardiac event-risks and probably to optimization of therapeutic strategy in patients with HFrEF.

## Keywords

cardiac sympathetic innervations • systolic heart failure • mechanical dyssynchrony • cardiac mortality • metaiodobenzylguanidine

\*Corresponding author. Tel: +81-0155-24-4161; Fax: +81-0155-25-7851. E-mail: doita518@yahoo.co.jp

Published on behalf of the European Society of Cardiology. All rights reserved. © The Author 2017. For permissions, please email: journals.permissions@oup.com.

## Introduction

Despite advances in evidence-based drug and/or non-pharmacological treatment, the morbidity and mortality of congestive heart failure are still high. Left ventricular mechanical dyssynchrony (LVMD) has emerged not only as a guide to cardiac resynchronization therapy (CRT) but also as a novel prognosis determinant in heart failure patients with reduced left ventricular ejection fraction (LVEF). Although CRT has been established as a non-pharmacological treatment in patients with advanced-stage heart failure that is refractory to conventional medical therapy,<sup>1,2</sup> about one-third of the patients who receive CRT do not respond to the treatment.<sup>3–5</sup> Rather than electrical dyssynchrony, increased mechanical LVMD is likely to be associated with lethal cardiac events and may be a better biomarker for CRT response.<sup>5</sup> Among several challenges for the evaluation of LVMD, a multicentre study failed to show the efficacy of echocardiographic LVMD assessment.<sup>6</sup> Phase analysis, which has been used traditionally to quantify global and regional temporal alterations of left ventricular systolic function, has recently been applied to gated single-photon emission computed tomography (SPECT) myocardial perfusion imaging for quantitative assessment of global LVMD.<sup>7–10</sup> Recent studies have demonstrated that LVMD assessed by gated SPECT imaging can be a biomarker not only for the indication of CRT but also for lethal cardiac event risks in patients with systolic heart failure.<sup>11–14</sup> On the other hand, cardiac sympathetic function and innervation can be evaluated using <sup>123</sup>I-labeled metaiodobenzylguanidine (MIBG) imaging as an increased norepinephrine spill-over (MIBG washout rate) and decreased norepinephrine content (MIBG activity) in failing human hearts. Recent multicentre investigations<sup>15–17</sup> definitively supported the earlier findings of the feasibility and prognostic values of cardiac <sup>123</sup>I-MIBG imaging for non-invasive quantitative assessment of cardiac sympathetic innervation in cardiology practice. The prognostic values of combined assessment of impairment of cardiac sympathetic innervation and LV dyssynchrony assessed by gated SPECT phase analysis, however, have not yet been established. The data reported previously are still preliminary because of small population studies, short-term studies and a lack of over-all evaluations such as the assessment of incremental prognostic values including standard prognostic markers in heart failure. From these findings, we hypothesized that cardiac mechanical dyssynchrony and cardioneuronal impairment are independently and synergistically related to unfavourable cardiac outcomes and can improve risk-stratification and risk-based selection of a therapeutic strategy for patients with heart failure. In this study, we investigated the interplay of LVMD assessed by gated SPECT imaging and impairment of cardiac sympathetic innervation assessed by cardiac <sup>123</sup>I-MIBG activity to clarify incremental prognostic implications in patients with chronic systolic heart failure when these prognostic biomarker are independently identified.

## Methods

### Study patients

A total of 570 consecutive patients with LVEF < 50% who were admitted with congestive heart failure symptoms were enrolled in this study. The patients included 415 (73%) males with a mean age of 67.0 ± 12.6 years

and a mean LVEF of 35.9 ± 10.7%. The diagnosis of heart failure at admission was established by clinical symptoms and signs according to the Framingham criteria including typical symptoms (palpitation, dyspnoea or orthopnoea), neck vein distension, peripheral oedema, lung rale, S3 or S4 gallop and tachycardia together with findings of chest X-ray and two-dimensional echocardiographic examinations such as cardiomegaly or left ventricular enlargement, bilateral lung congestion, pleural effusion, and left ventricular systolic dysfunction. Heart failure aetiologies such as ischaemic and non-ischaemic were established using a 12-lead electrocardiogram, echocardiography, and nuclear and/or angiographic examinations by excluding non-cardiac diseases showing similar symptoms and/or signs. Before enrolment to this study, 58 patients had undergone an implantable cardioverter defibrillator (ICD) treatment and 44 patients had undergone cardiac resynchronization therapy (CRT). Patients with overt malignancy, severe haemorrhagic diseases or neurological disorders such as Parkinson disease and Levy body dementia and patients undergoing treatment with tri-cyclic anti-depressants, reserpine, guanethidine, phenylpropranolamine and amphetamine, all of which inhibit cardiac <sup>123</sup>I-MIBG uptake, were excluded from this study. This study included 105 patients (18.4%) with end-stage renal failure undergoing haemodialysis. Blood examinations of haemoglobin (Hb), sodium, creatinine and brain natriuretic peptide (BNP) levels were done before discharge. Kidney function was evaluated as estimated glomerular filtration rate (eGFR) using the following formulas:  $eGFR = 194 \times \text{Cre}^{-1.094} \times \text{Age}^{-0.287}$  for males and  $eGFR = 0.739 \times \text{male eGFR}$  for females. Plasma BNP level was measured in the initial 175 patients (30.7%) and NT-pro BNP level was measured in the remaining 395 patients (69.3%). For statistical analysis of BNP and NT-pro BNP data, BNP and NT-pro BNP were classified into four stages based on the ESC guidelines for diagnosis and treatment of acute heart failure and chronic heart failure<sup>18</sup>: 0–40 pg/mL and 0–125 pg/mL for stage 1; 41–100 pg/mL and 126–400 pg/mL for stage 2; 101–200 pg/mL and 401–900 pg/mL for stage 3; and 201–pg/mL and 901–pg/mL for stage 4, respectively.

### Two-dimensional echocardiographic examination

Standard two-dimensional and pulsed Doppler echocardiographic study was performed by experienced echo-cardiographers who were blinded to clinical and scintigraphic data. Based on the American Society of Echocardiography recommendations, the following echocardiographic functional parameters were measured from apical four-, three-, and two-chamber views in a left lateral decubitus position using commercially available ultrasound machines equipped with a 2.5-MHz variable frequency transducer: left atrium diameter (LAD; mm), diastolic left ventricular diameter (LVDd; mm), diastolic ventricular septal wall thickness (IVSTd; mm), diastolic ventricular posterior wall thickness (PTWd; mm) in M-mode measurement, left ventricular ejection fraction (LVEF, %), left ventricular diastolic volume (EDV; mL), left ventricular systolic volume (ESV; mL) in 2D-measurement, E wave velocity (m/sec), left ventricular deceleration time (Dct; msec) and septal E/e'. LV volumes and LVEF were measured using the biplane modified Simpson's method. Echocardiographic data obtained in a stable condition before discharge were used for statistical analysis in this study.

### Cardiac <sup>123</sup>I-MIBG imaging

Following stabilization of the patient's condition, cardiac imaging with <sup>123</sup>I-MIBG of 111 MBq was performed using a gamma camera equipped with a low-energy, general-purpose collimator in a fasting and resting condition 15–30 min (early image) and 4 h (late image) after an intravenous tracer injection as described previously.<sup>16</sup> Cardiac <sup>123</sup>I-MIBG activity was measured as heart-to-mediastinum ratio (HMR) by a region of

interest being manually set on the upper mediastinum and the whole cardiac region on a planar anterior image by an experienced nuclear medicine technician without knowledge any clinical data.  $^{123}\text{I}$ -MIBG washout kinetics from the heart was calculated as washout rate (WVR) from the early and late cardiac  $^{123}\text{I}$ -MIBG activities without a decay correction.

## Assessment of cardiac mechanical dyssynchrony

Resting myocardial perfusion SPECT imaging with  $^{99\text{m}}\text{Tc}$ -tetrofosmin of 300 MBq was performed by an electrocardiography-gated approach with a frame rate of 16 using a single-head camera equipped with a high-resolution, parallel-hole collimator. Using the commercially available gated SPECT software 'Heart Function View (HFV version 1.1)',<sup>8</sup> LVMD was evaluated as a standard deviation (SD) of the regional onset-of-mechanical contraction phase angles (phase SD; unit, degrees) on a phase histogram created by Fourier phase analysis applied to regional time-activity curves obtained 3-dimensionally over the left ventricle (Figure 1).<sup>8–10</sup> This technique uses Fourier phase analysis to mathematically fit myocardial count changes depending on alterations of regional wall thickness over a cardiac cycle, which is basically identical to regional time-activity curves, for the calculation of regional phase angles of the curves on all SPECT slices over the left ventricle. Thus, a phase distribution map was expressed as a phase histogram and the degree of 3-dimensional LVMD was quantitatively evaluated as a phase SD on the phase map (Figure 1).

## Follow-up protocol

Following the enrolment in this study, patients were prospectively and regularly followed up by cardiologists with a primary endpoint of lethal cardiac events such as sudden cardiac death, death due to pump failure and appropriate ICD shock against life-threatening ventricular tachyarrhythmias, all of which had been defined prior to the start of this study, for at least 1 year when a patient survived. Patients' outcomes were clarified by reviewing medical records. Sudden cardiac death was defined as witnessed cardiac arrest and death within 1 h after onset of acute symptoms or unexpected death in patients known to have been well within the previous 24 h. This study was based on the principles outlined in the Declaration of Helsinki, and informed consent for enrolment in our database and usage for clinical study was obtained according to the guidelines of the ethics committee of our hospital.

## Statistical analysis

Each statistical value is shown as mean  $\pm$  1 standard deviation (SD). Mean values were compared between the two groups using the unpaired *t*-test, and categorical variables were compared using the chi-square test. Following univariate analysis, multivariate analysis with a Cox proportional hazard model was performed using the statistically appropriate number of significant variables identified by univariate analysis, which depended on the number of cardiac events. Receiver operating characteristic (ROC) analysis was performed to determine the optimal cutoff value of an independent significant parameter such as phase SD derived from gated SPECT and HMR of cardiac MIBG activity. Significant ( $P < 0.05$ ) determinants identified by univariate analysis were included in the multivariate models, and hazard ratios and 95% confidence intervals were estimated with the use of stratified Cox proportional hazards models. The Kaplan–Meier method was used to create time-dependent, cumulative event-free curves, which were compared using the log-rank test. For identification of incremental prognostic values of significant determinants, global chi-square values were calculated by combining several independent determinants determined by multivariable Cox analysis, based on increases in the overall likelihood ratio. A computer software program,

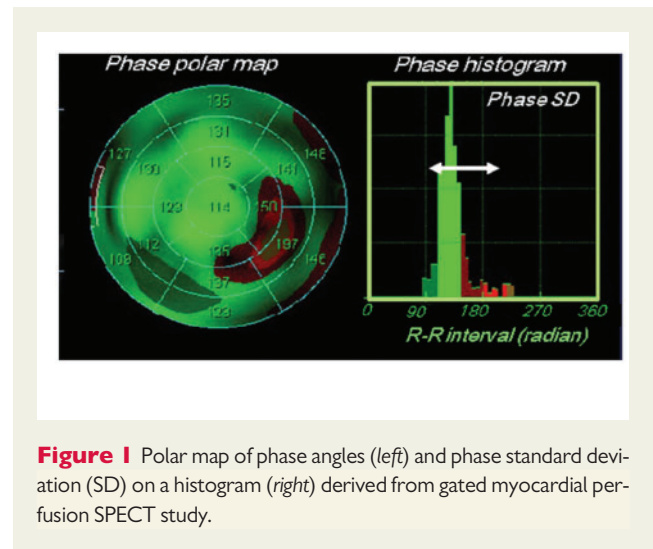


**Figure 1** Polar map of phase angles (left) and phase standard deviation (SD) on a histogram (right) derived from gated myocardial perfusion SPECT study.

SAS for Windows, version 9.4 (SAS Institute, Cary, North Carolina, USA), was used for these analyses. A *P*-value less than 0.05 was considered significant.

## Results

Primary endpoints were documented in 166 (29%) of the patients as follows: 143 patients died of pump failure, there were 12 sudden cardiac deaths and 11 patients experienced appropriate ICD shocks against lethal ventricular arrhythmias. Figure 2 shows two typical cases with and without a cardiac event.

The cardiac event group were older and had greater NYHA class, lower eGFR and significantly higher BNP/NT-pro BNP concentration than the non-cardiac event group (Table 1). Patients with cardiac events were more frequently treated with amiodarone, ICD than those without (Table 2). Despite the similar LVEFs, patients in the cardiac event group had a larger left atrium, shorter deceleration time, greater  $E/e'$ , significantly reduced cardiac MIBG activity (HMR) and greater phase SD than did patients in the non-cardiac event group: early HMR,  $1.63 \pm 0.30$  vs.  $1.75 \pm 0.26$ ,  $P < 0.0001$ ; late HMR,  $1.46 \pm 0.28$  vs.  $1.63 \pm 0.29$ ,  $P < 0.0001$ ; and  $39.1 \pm 11.6$  vs.  $33.1 \pm 10.1$ ,  $P < 0.0001$ ; respectively (Table 3).

Optimal cutoffs of late HMR and phase SD were determined by ROC analysis to be 1.54 and 38 degrees, respectively, for identifying high-risk patients. Patients with late HMR less than 1.54 or phase SD greater than 38 had significantly lower event-free rates than did other patients (Figure 3A and B). Likewise, when late HMR of 1.60 and phase SD of 60, both of which had been shown to be cutoffs in another study,<sup>14</sup> were applied to this study population, patients with lower late HMR or greater phase SD had significantly lower event-free rates than did other patients (Figure 3C and D). When classified into four subgroups using both late HMR and phase SD, patients with lower HMR and greater phase SD had the lowest event-free rate and, in contrast, patients with higher HMR and smaller phase SD had the highest event-free rate among the subgroups, independently of the definition of cutoff values (Figure 4). Among significant univariate variables (Table 4), the multivariate Cox proportional hazards model

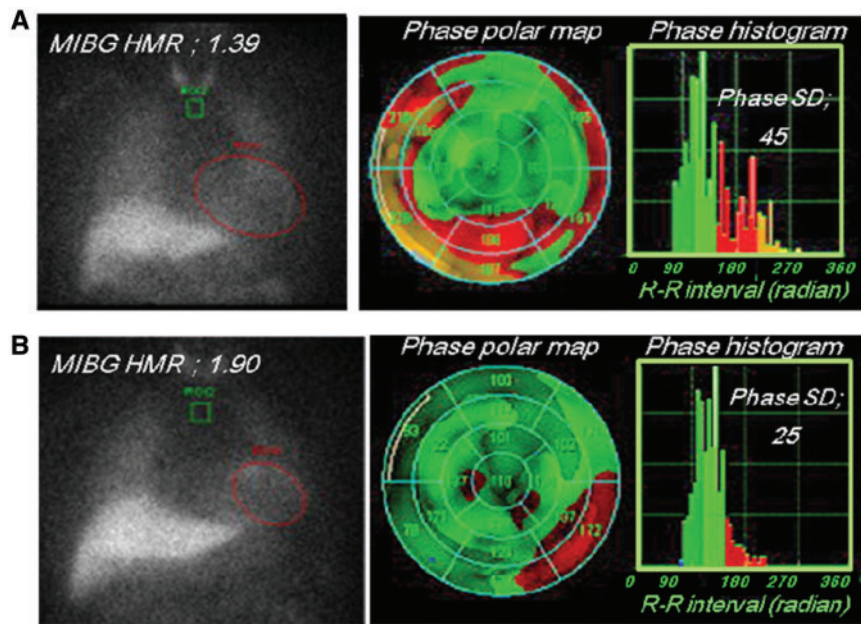


**Figure 2** Case demonstration. A 48-year-old man with NYHA class 2 heart failure, a very low heart-to-mediastinum ratio (HMR) (1.39) and a wide phase SD (45) died suddenly during the follow-up period. A 78-year-old man with NYHA class 1 heart failure, a mildly reduced HMR (1.90) and a relatively small phase SD (25) had no lethal cardiac event during the follow-up period.

**Table 1** Comparison of clinical data between groups with and without cardiac events

	Cardiac event group (n = 166)	Non-cardiac event group (n = 404)	P-value
Age (years old)	71.4±11.2	65.3±12.8	P < 0.0001
Gender (male/female)	126/40	289/115	P = 0.0004
Systolic blood pressure (mmHg)	111±20	120±18	P < 0.0001
NYHA (I/II/III/IV)	28/60/67/11	339/48/11/6	P < 0.0001
Past history			
Hypertension	83 (50.0%)	210 (51.9%)	ns
Diabetes mellitus	55 (33.1%)	154 (38.1%)	ns
Dyslipidaemia	54 (32.5%)	164 (40.5%)	ns
Atrial fibrillation	57 (34.3%)	134 (33.2%)	ns
Ventricular tachycardia/ventricular fibrillation	42 (25.3%)	71 (17.5%)	ns
Haemodialysis	39 (23.4%)	66 (16.3%)	ns
Aetiology, Ischaemic	78 (43.9%)	182 (45.0%)	ns
Device implantation			
ICD implantation	25 (15.1%)	33 (8.1%)	P = 0.0167
CRT implantation	16 (9.6%)	28 (6.9%)	ns
Laboratory data			
Haemoglobin (g/dL)	11.3±2.2	12.3±2.2	P < 0.0001
Creatinine (mg/dL)	3.2±3.2	2.6±2.1	P = 0.0001
eGFR (mL/min/1.73m <sup>2</sup> )	35.5±27.3	48.5±28.4	P < 0.0001
Sodium (mmol/L)	139.7±4.1	139.7±3.6	P = 0.0310
NT-pro BNP (pg/mL) (n = 395)	13612±21651	65713±20060	P = 0.0013
BNP (pg/mL) (n = 175)	1324±1650	492±604	P < 0.0001
Stagings of BNP and NT-pro BNP (1/2/3/4) (n = 570)	7/5/9/145	23/43/67/271	P < 0.0001

Values are shown as mean ± standard deviation. ICD, implantable cardioverter-defibrillator; CRT, cardiac Resynchronization Therapy; eGFR, Estimated glomerular filtration rate; NYHA, New York Heart Association Classification; BNP, Brain natriuretic peptide; NT-pro BNP, N-terminal pro-brain natriuretic peptide; ns, no significance.



**Table 2** Comparison of medications between groups with and without cardiac events

	Cardiac event group (n = 166)	Non-cardiac event group (n=404)	P-value
ACE-Is/ARBs	102 (61.4%)	234 (60.1%)	ns
Beta-adrenoceptor blocking agents	155 (93.3%)	366 (90.5%)	ns
Loop diuretics	126 (75.9%)	317 (78.4%)	ns
Aldosterone receptor antagonists	46 (27.7%)	123 (30.4%)	ns
Anti-vasopressin agents	30 (18.1%)	52 (12.9%)	ns
Calcium channel blockers	34 (20.5%)	112 (27.7%)	ns
Nitrates	27 (16.3%)	43 (10.6%)	ns
Amiodarone	41 (24.6%)	61 (15.1%)	P = 0.0028
Nicorangil	42 (25.3%)	135 (33.4%)	ns
Anti-platelet agents/Anti-coagulation agents	120(72.7%)	290 (71.9%)	ns
Statins	42(25.3%)	164 (40.6%)	P = 0.0004

ACE-Is, angiotensin-converting enzyme inhibitors; ARBs, angiotensin receptor blockers; ns, no significance.

**Table 3** Comparison of echocardiographic, cardiac sympathetic function, and dyssynchrony parameters between groups with and without cardiac events

	Cardiac event group (n = 166)	Non-cardiac event group (n = 404)	P-value
LVDd (mm)	55.3±11.2	55.2±9.1	ns
LVDs (mm)	46.0±12.4	44.9±10.1	ns
LAD (mm)	43.3±7.6	41.7±7.3	P = 0.0239
IVSTd (mm)	10.3±2.8	10.1±2.7	ns
PTWd (mm)	10.5±2.8	10.3±2.1	ns
Modified Simpson method			
LVEF (%)	34.6±12.3	36.4±10.1	ns
EDV(mL)	156.8±71.1	154.0±58.9	ns
ESV(mL)	107.3±66.3	98.8±52.2	ns
E wave velocity (m/sec)	0.85±0.29	0.83±0.29	ns
Dct (msec)	175.0±78.1	192.2±75.9	P = 0.0197
E/septal e'	20.3±8.2	17.9±6.9	P = 0.0007
E/septal e' (<15/15~)	50/116	180/224	P = 0.0264
Cardiac MIBG washout rate (%)	28.5±9.7	27.1±10.1	ns
Early HMR of MIBG activity	1.63±0.30	1.75±0.26	P < 0.0001
Late HMR of MIBG activity	1.46±0.28	1.63±0.29	P < 0.0001
Phase SD measured by gated SPECT	39.1±11.6	33.1±10.1	P < 0.0001

Values are shown as mean ± standard deviation (SD). LAD, left atrial diameter; LV, left ventricular; LVEF, left ventricular ejection fraction; LVDd, end-systolic left ventricular diameter; IVSTd, end-diastolic interventricular septal wall thickness; PWTd, end-diastolic posterior wall thickness; EDV, left ventricular end-diastolic volume; ESV, left ventricular end-systolic volume; Dct, left ventricular deceleration time; HMR, heart-to-mediastinum ratio; ns, no significance.

identified systolic blood pressure, NYHA functional class, eGFR, amiodarone use, late HMR of MIBG activity and phase SD as significant determinants of cardiac events with hazard ratios of 0.985 (CI, 0.975–0.995;  $P = 0.0037$ ), 2.268 (CI, 1.847–2.784;  $P < 0.0001$ ), 0.988 (CI, 0.980–0.995;  $P = 0.0021$ ), 1.958 (CI, 1.287–2.955;  $P = 0.0018$ ), 0.396 (CI, 0.215–0.712;  $P = 0.0020$ ) and 1.015 (CI, 1.009–1.041;  $P = 0.0330$ ), respectively. When combined with the four significant determinants (NYHA class, eGFR, late HMR, and phase SD) identified by Cox analysis, each prognostic power assessed by the global  $\chi^2$  value synergistically ( $P < 0.0001$ ) increased maximally up to 263.8 (Figure 5).

## Discussion

The results of the present study clearly showed that a global left ventricular systolic dyssynchrony identified by increased phase SD is not only a significant independent determinant of lethal cardiac events but also has incremental prognostic values in combination with impairment of cardiac sympathetic innervation and clinical information such as NYHA functional class and kidney function in heart failure patients.

Despite the definitive prognostic values of CRT in HFrEF patients with a wide QRS complex, nearly one third of HFrEF patients do not

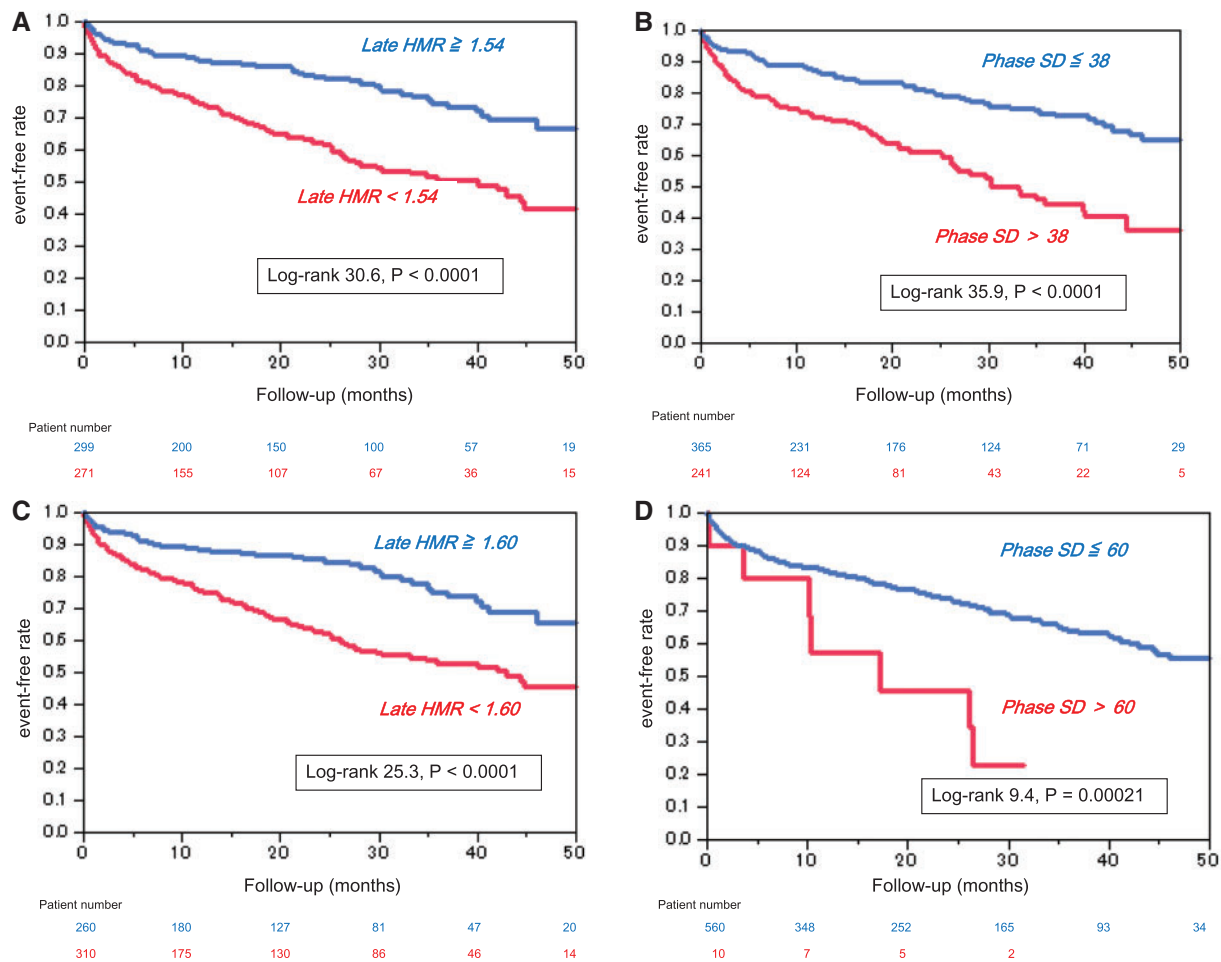


**Figure 3** Kaplan–Meier estimates of cardiac event-free survival stratified by late heart-to-mediastinum ratio (HMR) <math>< 1.54</math> (A) and phase SD > 38 (B), both of which were optimal cut-offs identified in this study, and late HMR <math>< 1.60</math> (C) and phase SD > 60 (D).

respond to CRT,<sup>3–5</sup> strongly suggesting the limitation of current CRT criteria using NYHA class III/IV, depressed LVEF and prolonged QRS duration (electrical dyssynchrony).<sup>5</sup> When compared to electrical dyssynchrony, global LVMD has several advantages. LVMD assessed by gated SPECT imaging with <sup>99m</sup>Tc-tetrofosmin reflects three-dimensional inhomogeneity in myocardial perfusion abnormality, cardiomyocyte injury and metabolic impairment (depletion of high-energy phosphate) of the myocardium, all of which result in heterogeneous electrophysiological instability, arrhythmogenicity and a loss of contractile force. Together with earlier findings,<sup>11–14,19</sup> the presented study demonstrated that LVMD is superior to conventional prognostic markers such as LVEF, BNP, and a wide QRS complex in heart failure<sup>20,21</sup> and is a powerful biomarker of temporal heterogeneity of contractile derangement responsible for lethal cardiac events. On the other hand, impairment of cardiac sympathetic innervation has been shown to be related to lethal outcomes in patients with heart failure undergoing pharmacological and ICD treatments independently of electrophysiological indices, LVEF, BNP, and myocardial

perfusion defect.<sup>22–29</sup> Similarly, the therapeutic response to CRT is likely to depend on cardiac sympathetic innervation assessed by cardiac MIBG activity.<sup>30–33</sup> Thus, combined assessment of LVMD and cardiac sympathetic innervation possibly improves identification of high-risk patients with heart failure who can most benefit from device therapy in a more appropriate risk-based and cost-effective manner.

As shown by a recent multiple cohort investigation,<sup>16</sup> assessment of cardiac sympathetic innervation using cardiac MIBG activity can precisely identify patients at low risk and at high risk for cardiac mortality over a period of 5 years or more, particularly when used in combination with standard clinical biomarkers such as age and NYHA functional class. The present study showed independent and incremental prognostic values of LVMD (increased phase SD > 38) and impairment of cardiac sympathetic function (reduced HMR of MIBG activity <math>< 1.54</math>) in HFrEF patients. The ADMIRE-HF sub-study using the propensity-matching<sup>14</sup> showed that phase SD > 60 and MIBG HMR <math>< 1.60</math> were significant and incremental determinants of sudden cardiac death in 170 patients with LVEF of 35% or less. The

**Table 4** Results of univariate and multivariate analyses

	Univariate analysis					
	$\chi^2$	Hazard ratio	95% CI		P-value	
			Lower	Upper		
Age	9.52	1.022	1.008	~	1.038	0.0020
Gender	4.51	0.636	0.402	~	0.967	0.0377
Systolic blood pressure	23.1	0.978	0.969	~	0.987	<0.0001
NYHA functional class	149.8	3.733	3.076	~	4.520	< 0.0001
Haemoglobin	18.9	0.859	0.803	~	0.920	< 0.0001
eGFR	30.1	0.984	0.978	~	0.989	< 0.0001
BNP+NT-pro BNP stage	13.5	1.519	1.201	~	1.989	0.0002
Amiodarone	30.2	2.746	1.932	~	3.891	< 0.0001
Statins	8.3	0.606	0.421	~	0.855	0.0040
Septal E/e'	18.4	1.050	1.027	~	1.073	< 0.0001
Late HMR	46.5	0.106	0.054	~	0.206	< 0.0001
Phase SD	30.1	1.048	1.029	~	1.062	< 0.0001
Multivariate Cox-hazard model analysis						
	$\chi^2$	Hazard ratio	95% CI		P-value	
			Lower	Upper		
Age	0.01	1.013	0.984	~	1.018	0.1153
Gender	4.14	0.659	0.442	~	1.043	0.0701
Systolic blood pressure	8.42	0.985	0.975	~	0.995	0.0037
NYHA functional class	58.8	2.268	1.847	~	2.784	< 0.0001
Haemoglobin	4.20	0.884	0.843	~	1.011	0.0516
eGFR	10.6	0.988	0.980	~	0.995	0.0021
BNP+NT-pro BNP stage	2.54	1.222	0.966	~	1.567	0.1104
Amiodarone	17.5	1.958	1.287	~	2.955	0.0018
Statins	0.28	0.896	0.598	~	1.327	0.5907
Septal E/e'	1.78	1.016	0.997	~	1.043	0.1814
Late HMR	15.1	0.396	0.215	~	0.712	0.0020
Phase SD	4.54	1.015	1.009	~	1.041	0.0330

CI, confidence interval; HMR, heart-to-mediastinum ratio; NYHA, New York Heart Association.

optimal cut-off values of HMR and LVMD determined by using ROC analysis in this study were smaller than those in the ADMIRE-HF sub-study. This is probably because there are differences in clinical back-grounds, patient number and method to determine cut-off values. Also when the ADMIRE-HF cut-off values were applied to our pa-tients, high-risk patients were clearly differentiated from the others. Besides the relatively short-term follow-up interval,<sup>14,15</sup> the number of high-risk patients identified by the ADMIRE-HF cut-off values were apparently smaller than that identified by our cut-off values (11 vs. 116, in Figure 5). From these findings, ROC-identified cut-off values of phase SD and HMR in this study are likely to more reasonably risk-stratify patients and to identify HFrEF patients at an increased risk for lethal cardiac events.

Phase SD derived from histogram analysis of multiple-gated myo-cardial perfusion data was used as a marker of LVMD in this study. This is because this parameter is quantified three-dimensionally using count-based data of mechanical contraction in the whole left

ventricle and is less affected by artefactual technical errors.<sup>8,14</sup> A high-ordered phase analysis of time-activity curves at each pixel has a high reproducibility and reliable quantitativity and can be standar-dized using an appropriate database for the assessment of global LVMD.<sup>8</sup> Gated myocardial perfusion SPECT imaging can be easily performed for the measurement of LVMD in conjunction with as-sessment of myocardial ischaemia and viability cardiac function with-out any additional cost or imaging time. On the other hand, a prolonged QRS complex is an electrical, but not mechanical, dyssyn-chrony index that is non-specific for heart failure pathophysiology and not necessarily related to impairment of cardiac function and heart failure outcomes, and the mechanisms have not been fully determined probably due to etiological diversity.<sup>34</sup>

Our previous studies<sup>16,35,36</sup> showed prognostic values of HF risk models using several significant determinants, including cardiac MIBG data. The recent ESC heart failure guidelines published in 2016 rec-ommend the Seattle Heart Failure Model<sup>37</sup> in combination with BNP

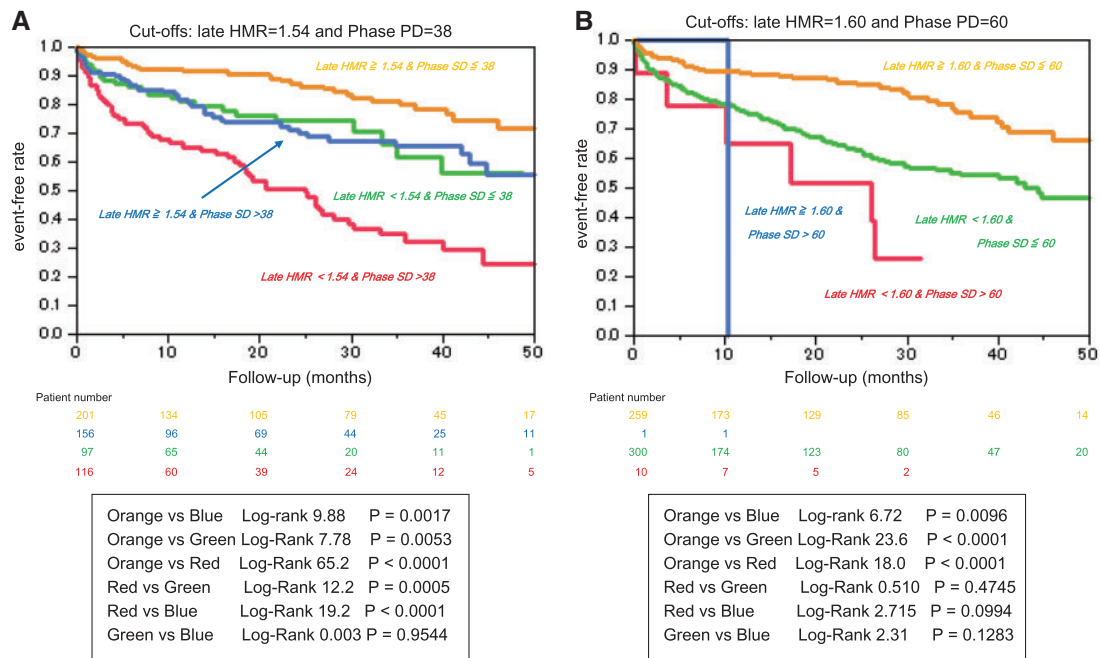


**Figure 4** Kaplan–Meier estimates of cardiac event-free survival stratified by the combination of late heart-to-mediastinum ratio (HMR) < 1.54 and phase SD > 38 (A) or late HMR < 1.60 and phase SD > 60 (B).

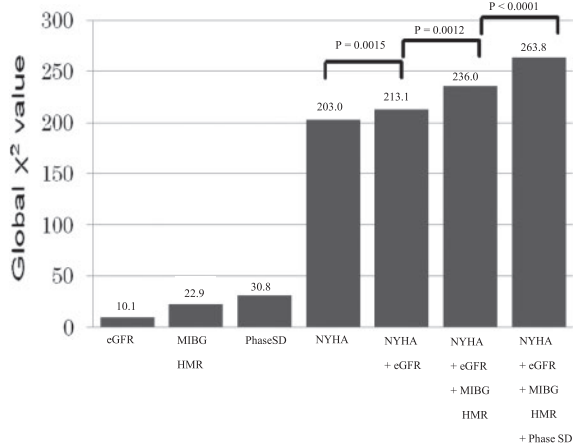


**Figure 5** Synergistic increases in prognostic powers assessed by global chi-square values using four determinants of cardiac events: NYHA functional class, estimated glomerular filtration rate (eGFR), late heart-to-mediastinum ratio (HMR) (1.54), and phase SD (38).

for the risk assessment of patients with HF<sub>r</sub>EF. In addition, Kuramoto *et al.*<sup>38</sup> showed the efficacy of cardiac MIBG imaging to improve the prognostic power of the Seattle heart failure model in patients with chronic heart failure. Although this study was not designed to

evaluate the Seattle heart failure model together with LVMD and cardiac sympathetic innervation, the presented results clarified the synergistic improvement in prognostic values of NYHA functional class, eGFR, LVMD, and MIBG activity (HMR). These findings strongly suggest further advance in a multiple-risk model using significant biomarkers mentioned above for more appropriate selection of therapeutic strategy in patients with HF<sub>r</sub>EF.

### Limitations and future perspectives

Since this study was a retrospective, observational study, a prospective multicentre study is needed particularly for the establishment of a risk-based therapeutic strategy using assessment of LVMD, cardiac sympathetic innervation and clinical variables presented here. As shown previously,<sup>26,28</sup> myocardial viability or perfusion abnormality are also important for predicting lethal cardiac event risk and benefits from ICD therapy. The extent and location of myocardial scar and LV lead position are determinants of the effectiveness of CRT together with LVMD.<sup>3–5</sup> Therefore, three-dimensional SPECT assessment of myocardial scar and viability possibly optimizes pacing lead placement and maximizes therapeutic response to CRT. It remains to be determined whether the combined assessment of LVMD and cardiac sympathetic innervation can predict a mode of death such as sudden cardiac death, death due to pump failure or both. Finally, because of limited medical resources and growing medical costs associated with out-patient care, recurrent hospitalization and widespread use of device therapy, there is a need to establish more cost-effective management of heart failure and more appropriate selection of device candidates using the methods presented here.



## Conclusions

Left ventricular mechanical dyssynchrony and impairment of cardiac sympathetic innervation are independently and synergistically related to lethal cardiac events. Their combined assessment can not only improve risk-stratification and prediction of lethal cardiac outcomes but also may contribute to maximizing clinical benefits of drug and device treatment in heart failure patients with reduced left ventricular ejection fraction.

## Acknowledgements

The authors sincerely thank the staff of the Nuclear Medicine Laboratory, Obihiro-Kosei General Hospital, Obihiro, Hokkaido, Japan, for cooperation with clinical services and their technical assistance.

**Conflict of interest:** None declared.

## References

- Sipahi I, Carrigan TP, Rowland DY, Stambler BS, Fang JC. Impact of QRS duration on clinical event reduction with cardiac resynchronization therapy: meta-analysis of randomized controlled trials. *Arch Intern Med* 2011;**171**:1454–62.
- Yancy CW, Jessup M, Bozkurt B, Butler J, Casey DE Jr, Drazner MH et al. 2013 ACCF/AHA guideline for the management of heart failure: a report of the American College of Cardiology Foundation/American Heart Association Task Force on Practice Guidelines. *J Am Coll Cardiol* 2013;**62**:e147–239.
- Abraham WT, Fisher WG, Smith AL, Delurgio DB, Leon AR, Loh E et al. Cardiac resynchronization in chronic heart failure. *N Engl J Med* 2002;**346**:1845–53.
- Fox DJ, Fitzpatrick AP, Davidson NC. Optimization of cardiac resynchronization therapy: addressing the problem of “non-responders”. *Heart* 2005;**91**:1000–2.
- Chung ES, Leon AR, Tavazzi L, Sun JP, Nihoyannopoulos P, Merlino J et al. Results of the predictors of response to CRT (PROSPECT) trial. *Circulation* 2008;**117**:2608–16.
- Hawkins NM, Petrie MC, Burgess MI, McMurray JJ. Selecting patients for cardiac resynchronization therapy: the fallacy of echocardiographic dyssynchrony. *J Am Coll Cardiol* 2009;**53**:1944–59.
- Chen J, Garcia EV, Folks RD, Cooke CD, Faber TL, Tauxe EL et al. Onset of left ventricular mechanical contraction as determined by phase analysis of ECG-gated myocardial perfusion SPECT imaging: development of a diagnostic tool for assessment of cardiac mechanical dyssynchrony. *J Nucl Cardiol* 2005;**12**:687–95.
- Nakajima K, Okuda K, Matsuo S, Kiso K, Kinuya S, Garcia EV. Comparison of phase dyssynchrony analysis using gated myocardial perfusion imaging with four software programs: Based on the Japanese Society of Nuclear Medicine working group normal database. *Nucl Cardiol* 2016. [Epub ahead of print]
- Chen J, Henneman MM, Trimble MA, Bax JJ, Borges-Neto S, Iskandrian AE et al. Assessment of left ventricular mechanical dyssynchrony by phase analysis of ECG-gated SPECT myocardial perfusion imaging. *J Nucl Cardiol* 2008;**15**:127–36.
- Atchley AE, Kitzman DW, Whellan DJ, Iskandrian AE, Ellis SJ, Pagnanelli RA et al. Myocardial perfusion, function, and dyssynchrony in patients with heart failure: baseline results from the single-photon emission computed tomography imaging ancillary study of the Heart Failure and A Controlled Trial Investigating Outcomes of Exercise TraiNing (HF-ACTION) Trial. *Am Heart J* 2009;**158**:S53–63.
- Pazhenkottil AP, Buechel RR, Husmann L, Nkoulou RN, Wolfrum M, Ghadri JR et al. Long-term prognostic value of left ventricular dyssynchrony assessment by phase analysis from myocardial perfusion imaging. *Heart* 2011;**97**:33–7.
- Wang L, Yang MF, Cai M, Zhao SH, He ZX, Wang YT. Prognostic significance of left ventricular dyssynchrony by phase analysis of gated SPECT in medically treated patients with dilated cardiomyopathy. *Clin Nucl Med* 2013;**38**:510–5.
- Zafir N, Nevzorov R, Bental T, Strasberg B, Gutstein A, Mats I et al. Prognostic value of left ventricular dyssynchrony by myocardial perfusion-gated SPECT in patients with normal and abnormal left ventricular functions. *J Nucl Cardiol* 2014;**21**:532–40.
- Hage FG, Aggarwal H, Patel K, Chen J, Jacobson AF, Heo J et al. The relationship of left ventricular mechanical dyssynchrony and cardiac sympathetic denervation to potential sudden cardiac death events in systolic heart failure. *J Nucl Cardiol* 2014;**21**:78–85.
- Jacobson AF, Senior R, Cerqueira MD, Wong ND, Thomas GS, Lopez VA et al. Myocardial iodine-123 meta-iodobenzylguanidine imaging and cardiac events in chronic heart failure. Results of the prospective ADMIRE-HF (AdreView myocardial imaging for risk evaluation in heart failure) study. *J Am Coll Cardiol* 2010;**55**:2212–21.
- Nakata T, Nakajima K, Yamashina S, Yamada T, Momose M, Kasama S et al. A pooled analysis of multicenter cohort studies of I-123-mIBG cardiac sympathetic innervation imaging for assessment of long-term prognosis in chronic heart failure. *J Am Coll Cardiol Cardiovasc Imaging* 2013;**6**:772–84.
- Verschure DO, Veltman CE, Manrique A, Somsen GA, Koutelou M, Katsikis A et al. For what endpoint does myocardial 123I-MIBG scintigraphy have the greatest prognostic value in patients with chronic heart failure? Results of a pooled individual patient data meta-analysis. *Eur Heart J Cardiovasc Imaging* 2014;**15**:996–1003.
- McMurray JJ, Adamopoulos S, Anker SD, Auricchio A, Böhm M, Dickstein K et al. ESC Guidelines for the diagnosis and treatment of acute and chronic heart failure 2012: The Task Force for the Diagnosis and Treatment of Acute and Chronic Heart Failure 2012 of the European Society of Cardiology. Developed in collaboration with the Heart Failure Association (HFA) of the ESC. *Eur Heart J* 2012;**33**:1787–847.
- Chen J, Garcia EV, Bax JJ, Iskandrian AE, Borges-Neto S, Soman P. SPECT myocardial perfusion imaging for the assessment of left ventricular mechanical dyssynchrony. *J Nucl Cardiol* 2011;**18**:685–94.
- Bhatia RS, Tu JV, Lee DS, Austin PC, Fang J, Haouzi A et al. Outcome of heart failure with preserved ejection fraction in a population-based study. *N Engl J Med* 2006;**355**:260–9.
- Hunt SA, Abraham WT, Chin MH, Feldman AM, Francis GS, Ganiats TG et al. 2009 Focused update incorporated into the ACC/AHA 2005 Guidelines for the Diagnosis and Management of Heart Failure in Adults. A Report of the American College of Cardiology Foundation/American Heart Association Task Force on Practice Guidelines Developed in Collaboration with the International Society for Heart and Lung Transplantation. *J Am Coll Cardiol* 2009;**53**:e1–e90.
- Nakata T, Wakabayashi T, Kyuma K, Takahashi T, Tsuchihashi K, Shimamoto K. Cardiac metaiodobenzylguanidine activity can predict the long-term prognostic efficacy of angiotensin-converting enzyme inhibitors and/or beta-adrenoceptor blockers in patients with heart failure. *Eur J Nucl Med Mol Imaging* 2005;**32**:186–94.
- Nakajima K, Nakata T. Cardiac 123I-MIBG imaging for clinical decision making: 22-year experience in Japan. *J Nucl Med* 2015;**56** Suppl 4:115–19S. doi: 10.2967/jnumed.114.142794.
- Arora R, Ferrick KJ, Nakata T, Kaplan RC, Rozengarten M, Latif F et al. I-123 MIBG imaging and heart rate variability analysis to predict the need for an implantable cardioverter defibrillator. *J Nucl Cardiol* 2003;**10**:121–31.
- Nagahara D, Nakata T, Hashimoto A et al. Predicting the need for an implantable cardioverter defibrillator using cardiac metaiodobenzylguanidine activity together with plasma natriuretic peptide concentration or left ventricular function. *J Nucl Med* 2008;**49**:225–33.
- Nishisato K, Hashimoto A, Nakata T, Doi T, Yamamoto H, Nagahara D et al. Impaired cardiac sympathetic innervation and myocardial perfusion are related to lethal arrhythmia: quantification of cardiac tracers in patients with ICDs. *J Nucl Med* 2010;**51**:1241–9.
- Boogers MJ, Borleffs CJ, Henneman MM, van Bommel RJ, van Ramshorst J, Boersma E et al. Cardiac sympathetic denervation assessed with 123I-iodine metaiodobenzylguanidine imaging predicts ventricular arrhythmias in implantable cardioverter-defibrillator patients. *J Am Coll Cardiol* 2010;**55**:2769–77.
- Sood N, Al Badarin F, Parker M, Pullatt R, Jacobson AF, Bateman TM et al. Resting perfusion MPI-SPECT combined with cardiac 123I-mIBG sympathetic innervation imaging improves prediction of arrhythmic events in non-ischemic cardiomyopathy patients: sub-study from the ADMIRE-HF trial. *J Nucl Cardiol* 2013;**20**:813–20.
- Aljaroudi WA, Hage FG, Hermann D, Doppalapudi H, Venkataraman R, Heo J et al. Relation of left-ventricular dyssynchrony by phase analysis of gated SPECT images and cardiovascular events in patients with implantable cardiac defibrillators. *J Nucl Cardiol* 2010;**17**:398–404.
- Nishioka SA, Martinelli Filho M, Brandão SC, Giorgi MC, Vieira ML, Costa R et al. Cardiac sympathetic activity pre and post resynchronization therapy evaluated by 123I-MIBG myocardial scintigraphy. *J Nucl Cardiol* 2007;**14**:852–9.
- Cha YM, Oh J, Miyazaki C, Hayes DL, Rea RF, Shen WK et al. Cardiac resynchronization therapy upregulates cardiac autonomic control. *J Cardiovasc Electrophysiol* 2008;**19**:1045–52.
- Burri H, Sunthorn H, Somsen A, Fleury E, Stettler C, Shah D et al. Improvement in cardiac sympathetic nerve activity in responders to resynchronization therapy. *Europace* 2008;**10**:374–8.
- Shinohara T, Takahashi N, Saito S, Okada N, Wakisaka O, Yufu K et al. Effect of cardiac resynchronization therapy on cardiac sympathetic nervous dysfunction and serum C-reactive protein level. *Pacing Clin Electrophysiol* 2011;**34**:1225–30.
- Eschaliér R, Ploux S, Ritter P, Haïssaguerre M, Ellenbogen KA, Bordachar P. Nonspecific intraventricular conduction delay: Definitions, prognosis, and implications for cardiac resynchronization therapy. *J Heart Rhythm* 2015;**12**:1071–9.

35. Nakajima K, Nakata T, Yamada T, Yamashina S, Momose M, Kasama S *et al*. A prediction model for 5-year cardiac mortality in patients with chronic heart failure using I-123 meta-iodobenzylguanidine imaging. *Eur J Nucl Med Mol Imaging* 2014;**41**:1673–82.
36. Nakajima K, Nakata T, Matsuo S, Jacobson AF. Creation of mortality risk charts using 123I meta-iodobenzylguanidine heart-to-mediastinum ratio in patients with heart failure: 2- and 5-year risk models. *Eur Heart J Cardiovasc Imaging* 2016;**17**:1138–45.
37. AbouEzzedine OF, French B, Mirzoyev SA, Jaffe AS, Levy WC, Fang JC *et al*. From statistical significance to clinical relevance: a simple algorithm to integrate brain natriuretic peptide and the Seattle Heart Failure Model for risk stratification in heart failure. *J Heart Lung Transplant* 2016;**35**:714–21.
38. Kuramoto Y, Yamada T, Tamaki S, Okuyama Y, Morita T, Furukawa Y *et al*. Usefulness of cardiac iodine-123 meta-iodobenzylguanidine imaging to improve prognostic power of Seattle heart failure model in patients with chronic heart failure. *Am Heart J* 2011;**107**:1185–90.

## IMAGE FOCUS

doi:10.1093/ehjci/jex228  
Online publish-ahead-of-print 16 October 2017

# A crown of thorns—right ventricular outflow tract obstruction caused by calcific pericardial ring

Ee Ling Heng<sup>1,2</sup>, Thomas Semple<sup>3\*</sup>, Konstantinos Dimopoulos<sup>1</sup>, Edward D. Nicol<sup>3</sup>, and Raad H. Mohiaddin<sup>2</sup>

<sup>1</sup>Department of Adult Congenital Heart Disease, The Royal Brompton Hospital, Sydney Street, SW3 6NP, London, UK; <sup>2</sup>Department of Cardiac MRI, Royal Brompton Hospital, National Heart and Lung Institute, Imperial College London, UK; and <sup>3</sup>Department of Radiology, The Royal Brompton Hospital, Sydney Street, SW3 6NP, London, UK

\* Corresponding author. Tel: +442073528121; Fax: +442073528098. E-mail: tsemple@doctors.org.uk

A 56-year-old asymptomatic Caucasian male was referred for cardiac review after incidental detection of a systolic praecordial murmur. Clinical examination elicited a right ventricular (RV) heave, split second heart sound and soft, ejection systolic murmur at the sternal edge. Echocardiography and Cardiac Magnetic Resonance Imaging (CMR) revealed mild sub-pulmonary RV outflow tract (RVOT) obstruction (peak RVOT gradient 15 mmHg) with relative post-obstructive main pulmonary artery dilatation. Biventricular size and function were normal. There were no Doppler features of constriction, although diastolic septal bounce was noted. The estimated right ventricular systolic pressure was 21 mmHg. Cardiac computed tomography (*Panel A*) confirmed the presence of an encircling calcific band at the level of the atrioventricular groove (also visible on chest radiography, *Panel B*), causing static extrinsic RVOT compression (see Supplementary data online, *Video S1*). No coronary calcification or impingement was demonstrated. Calcified pulmonary granulomata were noted (*Panel C*), in keeping with previous tuberculosis as the likely aetiology—subsequently confirmed. The patient has been managed conservatively with serial surveillance in view of the mild haemodynamic impact of the pericardial ring.

Calcific pericardial rings are most commonly the sequelae of chronic tuberculous constrictive pericarditis and appear to preferentially occur over the lower pressure right heart chambers and the atrioventricular grooves. Other causes of calcific pericarditis include previous pericardiectomy, congenital heart disease, infection, sarcoidosis, and radiation. Dense, calcified rings can cause extrinsic compression of intra-cardiac structures and the great vessels; as well as coronary artery obstruction. Definitive management involves surgical pericardiectomy, and long-term follow-up is mandated post-operatively due to the risk of recurrence.

Supplementary data are available at *European Heart Journal—Cardiovascular Imaging* online.

Published on behalf of the European Society of Cardiology. All rights reserved. © The Author 2017. For permissions, please email: journals.permissions@oup.com.

